13th World Conference on Earthquake Engineering
Vancouver, B.C., Canada
August 1-6, 2004
Paper No. 3102

VULNERABILITY ANALYSIS OF FLAT SLAB STRUCTURES

M. Altug ERBERIK[1], Amr S. ELNASHAI[2]

SUMMARY

Flat-slab RC buildings exhibit several advantages over conventional moment-resisting frames. However the structural effectiveness of flat-slab construction is hindered by its alleged inferior performance under earthquake loading. This is a possible reason for the observation that no fragility analysis has been undertaken for this widely-used structural system. This study focuses on the derivation of fragility curves using medium-rise flat-slab buildings with masonry infill walls. The developed curves were compared with those in the literature, derived for moment-resisting RC frames. The study concluded that earthquake losses for flat-slab structures are in the same range as for moment-resisting frames for low limit states, and considerably different at high damage levels. Observed differences are justifiable on the grounds of structural response characteristics of the two structural forms.

INTRODUCTION

Seismic loss assessment depends on the comprehensive nature of estimating vulnerability. The determination of vulnerability measure requires the assessment of the seismic performances of all types of building structures typically constructed in an urban region when subjected to a series of earthquakes, taking into account the particular response characteristics of each structural type. The fragility study generally focuses on the generic types of construction because of the enormity of the problem. Hence simplified structural models with random properties to account for the uncertainties in the structural parameters are used for all representative building types.

The flat-slab system is a special structural form of reinforced concrete construction that possesses major advantages over the conventional moment-resisting frames (Figure 1). The former system provides architectural flexibility, unobstructed space, lower building height, easier formwork and shorter construction time. There are however, some serious issues that require examination with the flat-slab construction system. One of the issues which were observed is the potentially large transverse displacements because of the absence of deep beams and/or shear walls, resulting in low transverse stiffness. This induces excessive deformations which in turn causes damage of non-structural members even when subjected to earthquakes of moderate intensity. Another issue is the brittle punching failure due to the transfer of shear forces and unbalanced moments between slabs and columns. Flat-slab systems

[1] Department of Civil Engineering, Middle East Technical University, Ankara 06531, Turkey.
[2] Willett Professor of Engineering, Department of Civil and Environmental Engineering, University of Illinois at Urbana-Champaign IL 61801 USA

are also susceptible to significant reduction in stiffness resulting from the cracking that occurs from construction loads, service gravity loads; temperature and shrinkage effects and lateral loads. Therefore, it was recommended that in regions with high seismic hazard, flat-slab construction should only be used as the vertical load carrying system in structures braced by frames or shear walls responsible for the lateral capacity of the structure (ACI-ASCE Committee [1]). However, flat-slab systems are often adopted as the primary lateral load resisting system and their use has proven popular in seismically active regions, such as in the Mediterranean basin. In these cases, the design of flat-slab buildings is typically carried out in a manner similar to ordinary frames. Where the latter practice is followed, the response under moderate earthquakes indicates extensive damage to non-structural elements even when the code provisions for drift limitation are satisfied (Chow and Selna [2]). This observation emphasizes the necessity of investigating the vulnerability of flat-slab construction, for which no fragility curves are available in the literature, since the structure exhibits distinct response modes, as compared to conventional moment-resisting frames.

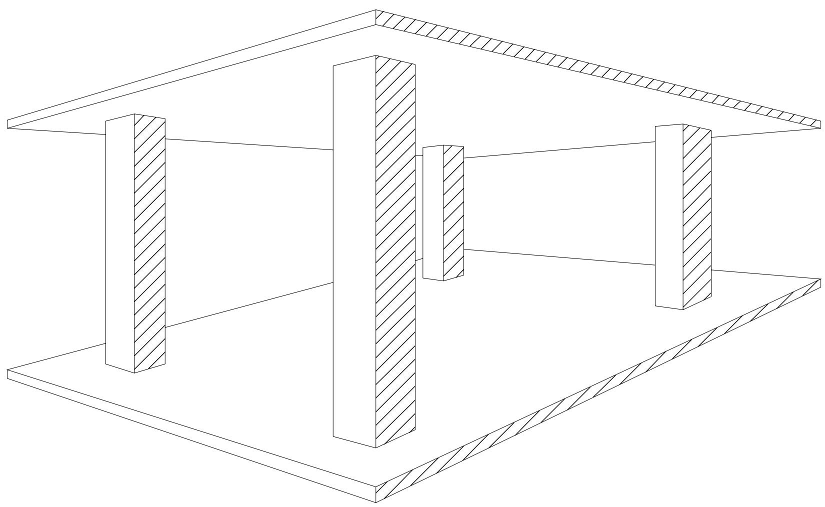

Figure 1. Illustration of a typical flat-slab structural form

METHODOLOGY FOR DEVELOPING FRAGILITY CURVES

In the construction of the fragility functions, there is no definitive method or strategy (Wen et al., 2003 [3]). A great degree of uncertainty is involved in each step of the procedure. This uncertainty is due to variability in ground motion characteristics, analytical modeling, materials used and definition of the limit states. The current study employs accepted procedures whilst attempting to ensure that rational decisions are taken along the route to deriving vulnerability curves for a structural system that has not been dealt with before. The approach used is outlined in Figure 2. A detailed account is given hereafter of the various steps depicted in Figure 2.

Structural Configuration and Design

A five story (mid-rise) flat slab structure is used as the generic system for this study. The reason for choosing a mid-rise building is two-fold. Because of the inherent flexibility of flat-slab buildings, it may not be possible to satisfy the drift demands in high-rise construction. On the other hand, low-rise buildings would be sufficiently stiff and may not warrant special consideration. The selected dimensions of the building are shown in Figure 3. For simplicity, the building is symmetric in plan with three bays in the horizontal direction. This symmetry enables the use of 2-D models in both design and analysis.

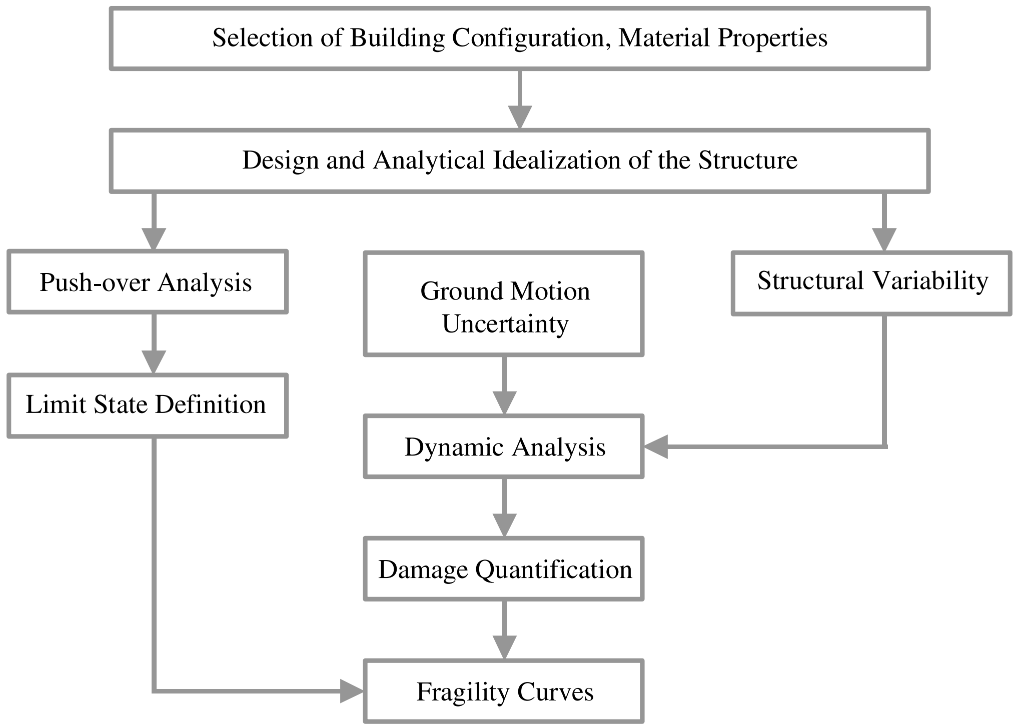

Figure 2. The methodology employed for the development of fragility curves

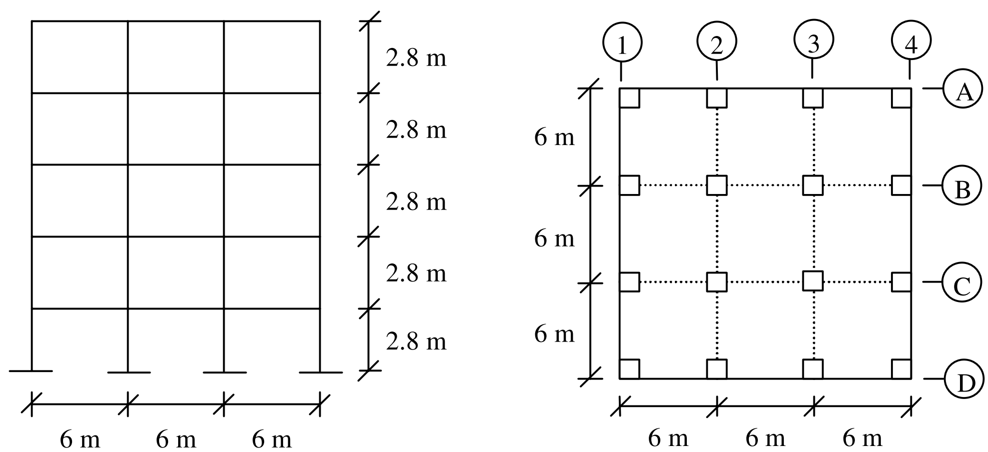

Figure 3. Five-story flat-slab building in elevation and in plan

The building was designed according to the regulations of ACI 318-99 [4]. Following common practices, the materials used are 4000 psi (28 MPa) concrete and Grade 60 (414 MPa) reinforcing bars. The gravity load scenario consists of dead load and live load. The seismic design is carried out according to FEMA 368, NEHRP Recommended Provisions for Seismic Regulations for New Buildings and Other Structures (Building Seismic Safety Council [5]). The flat-slab building is assumed to be located in Urbana, IL.

The direct design approach was used to determine the slab reinforcement. Since the most significant problem of flat-slab system is the punching shear failure, precautions should be taken in the design stage to prevent this undesirable behavior. The depth of the slab was selected according to the requirements in the code to prevent this type of failure. The slab-beams' reinforcement was detailed to prevent slab failure caused by the combination of forces, including shear, torsion and moment transferred from the column. The bottom reinforcement of the slab was continuous with a reasonable amount passing through the columns. This prevented the progressive vertical collapse of slabs in the event of a local punching failure. The column dimensions used were 40 cm x 40 cm throughout the height of the building. Longitudinal and lateral reinforcement were determined according to the ACI regulations.

Development of the Analytical Model

In this study, the building is modeled as a 2-D planar frame with lumped masses. ZEUS-NL; Elnashai et al. [6], is the software program used for the inelastic analysis of the flat-slab structure. The program is a development of previous analytical platforms developed at Imperial College, namely ADAPTIC and INDYAS. In order to model the slabs, the portion that will contribute to the frame analysis should be determined as well as the width of the concealed beam within the slab. For the flat-slab structure being studied, the portion of the slab that will contribute to the frame analysis is determined by using the formulations proposed by Luo and Durrani [7].

The control of the excessive drift in the flat-slab structure is maintained by the masonry infill walls, which have high in-plane stiffness. The infilled frame is modeled as an equivalent diagonally braced frame, where masonry infill walls are represented by diagonal compression struts.

The concrete is modeled by using the inelastic concrete model with constant (active) confinement in ZEUS-NL. Steel is modeled with a bilinear elasto-plastic model with kinematic strain-hardening. Further detail in relation to the development stage of the analytical model can be found elsewhere (Erberik [8]).

Selection of Ground Motion Records

Since the current study focuses on the effects of the ground motion variability on the building response, there should be a compromise between the number of ground motions selected and the robustness of the analysis. Bazzuro and Cornell [9] suggested that five-to-seven input motions are sufficient for the representing the hazard in an uncoupled (uncertainty in supply and demand dealt with separately) analysis. Dymiotis et al. [10] states that three ground motions are sufficient if appropriate choices of records and scaling are made. Taking the latter studies into consideration, ten ground motions with a single criterion; the compatibility of the elastic spectra of these ground motions with the code spectrum used in the seismic design of the building, were selected. The selected ground motions and their characteristics are listed in Table 1.

Evaluation of Seismic Response Characteristics

Before conducting inelastic dynamic analyses to for the development of fragility curves of the flat-slab structure, it is necessary to assess the structural response characteristics through eigenvalue and the inelastic static (pushover) analyses. In the eigenvalue analysis, the first three natural periods of the structure are obtained as T=0.38, 0.13 and 0.08 seconds, respectively. The natural vibration periods seemed reasonable for mid-rise concrete frames with infill panels.

The static pushover analysis was conducted using the ZEUS-NL. An inverted triangular distribution was used for the lateral loading. Force-controlled analysis was chosen to identify the structural deficiencies of the frame, such as soft stories. The frame was capable of sustaining a lateral load of 1056 kN (0.25% of the weight of the frame).

Table .1 Characteristics of the selected ground motions

No	*Location*	*Comp*	*Earthquake*	*Country*	*Year*	M_s	*PGA* (m/s^2)	$S_{a,max}$ *(g)*
1	Buia	NS	Friuli Aftershock	Italy	1976	6.1	1.069	0.327
2	Boshroyeh	N79E	Tabas	Iran	1978	7.3	1.004	0.339
3	Cassino Sant'Elia	EW	Lazio Abruzzo	Italy	1984	5.8	1.116	0.395
4	Gukasian	NS	Spitak	Armenia	1988	5.8	1.446	0.395
5	Hayward-Muir Sch.	90	Loma Prieta	USA	1989	7.1	1.360	0.454
6	Tonekabun	EW	Manjil	Iran	1990	7.3	0.871	0.302
7	LA-Govt. Off. Bldg.	270	Northridge	USA	1994	6.7	1.367	0.362
8	El Segundo-Off. Bldg.	90	Northridge	USA	1994	6.7	1.281	0.362
9	Castelmuovo-Assisi	EW	Umbro-Marchigiano	Italy	1997	5.5	1.083	0.405
10	Yesilkoy Airport	NS	Marmara	Turkey	1999	7.8	0.871	0.366

Determination of Limit States

Definition of limit states plays a significant role in the construction of the fragility curves. Well-defined and realistic limit states are of paramount importance since these values have a direct effect on the fragility curve parameters. This is especially true for special systems like flat-slab structures for which the identification of limit states is highly dependent on the characteristics of the structure. It may be misleading to use the performance levels determined for regular concrete frames in the case of the flat-slab buildings without due regard to the inherent flexibility of these structures.

The limit states used in this study are defined in terms of interstory drift ratio since the behavior and the failure modes of such structures are governed by deformation. To determine performance levels, the local limit states of members in an individual story are obtained and then mapped onto the shear force vs. drift curve of that story. Local limit states are considered in terms of yield and ultimate curvatures. Then these performance points are used to obtain the limit states of the story in terms of interstory drift. This process is repeated for each story. The performance levels of the most critical story are defined as the global limit states of the structure. The global limit state is illustrated in Figure 4.a for the first story of the analysis model used. In this figure, hollow rectangular marks represent the failure of the diagonal struts used to simulate the infill panels, solid circular marks denote the local yield criterion and hollow triangular marks represent local ultimate criterion. The yield and ultimate limit state occurrences in the structural members of the first story are illustrated in Figure 4.b and 4.c. When comparing the story shear versus drift curve, it is observed that the infill panels fail sequentially at a low drift level of 3.5 mm. After the failure of the infill panels, the stiffness is significantly reduced. At a drift level of 25-30 mm, the yield limit state is reached at the left end of three beams (Y1) followed by the bottom end of three first story columns (Y2). Two more yield limit states (Y3, Y4) occur at a drift level of approximately 60 mm, in addition to exceeding the ultimate state in one of the beams (U1). At a drift level of 100 mm, the ultimate limit state is exceeded in three columns (U2). Considering this limit state scenario and verifying that the most critical story drifts take place in the first story, the limit states assigned to the frame in terms of interstory drift are shown in Table 2.

Material Uncertainty

One of the main sources that control the response uncertainty of a reinforced concrete structure is the inherent variability of material strength. The mean and standard deviation are used to describe the statistical variation of the material properties. Normal or lognormal distributions are commonly used, for convenience. In this study, the yield strength of steel and the compressive strength of concrete have been chosen as the random variables following a survey of the literature (e.g. Dymiotis et al [10]) and pilot inelastic analysis using extreme values of material properties.

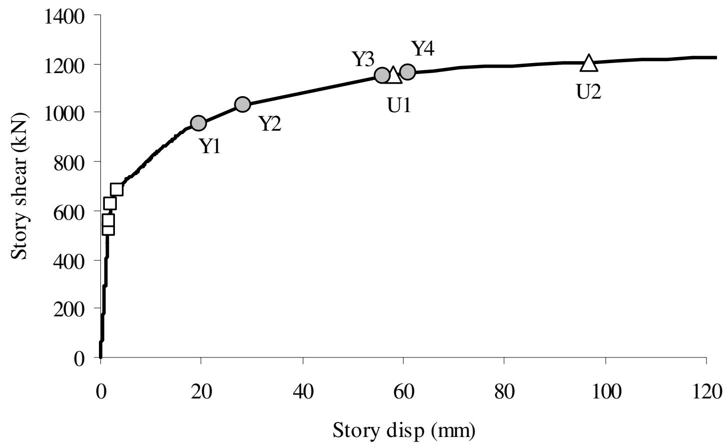

a) Story shear vs. story drift curve

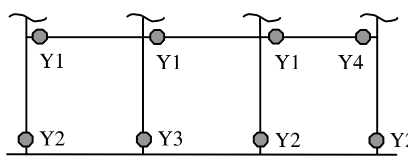

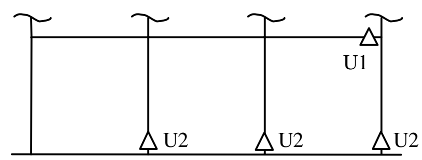

b) Yield Limit State

c) Ultimate Limit State

Figure 4. Mapping from local limit states to global limit states

Table 2 Limit states and corresponding interstory drift ratios

Limit State	*Interstory Drift (mm)*	*Interstory Drift Ratio (%)*
Slight	3.5	0.1
Moderate	28.4	1.0
Extensive	56.1	2.0
Complete	96.9	3.5

A lognormal distribution is assumed for the yield strength of steel in this study. The mean and COV are 475 MPa and 6 %, respectively. Hence the lognormal mean and standard deviation parameters take the values of 6.161 and 0.06, respectively. To represent the variability of concrete strength, a normal distribution is employed. For a characteristic concrete strength value of 28 MPa, the mean value is calculated as 36 MPa and COV is taken as 15%.

Treatment of Material Uncertainty - Sampling

In this study, Latin Hypercube Sampling (LHS) Technique is employed. This technique provides a constrained sampling scheme instead of the random sampling used in the Monte Carlo Method. Therefore it is possible to use a rather small sample size to achieve the required accuracy.

The variability of the yield strength of steel reinforcement in beams and columns is treated separately. Hence three sets of input values are generated to represent the variability in the compressive strength of concrete, the yield strength of steel reinforcement in beams and the yield strength of steel reinforcement in columns. The variables are indicated as f_c, $f_{y,b}$ and $f_{y,c}$, respectively. Thirty sets of input data are generated to use in the simulation of the dynamic response of the flat-slab structure. To achieve this, the range of each random variable is divided into thirty non-overlapping intervals on the basis of equal probability. One value from each interval is selected randomly with respect to the probability density in the interval. Thus the thirty values obtained for f_c are paired randomly with the thirty values of $f_{y,b}$. These thirty pairs are further combined with the thirty values of $f_{y,c}$ to form thirty sets of input data for the response simulation analyses. The employment of the LHS Method to develop detailed fragility curves of flat-slab structures is described in Erberik [8].

Seismic Response Analysis

Inelastic response-history analysis is used to evaluate the seismic response and to derive the fragility curves. This method is actually the most tedious one but it is also the most direct and accurate way to generate the fragility functions of building structures.

Spectral displacement (S_d) is used as the hazard parameter for constructing the fragility curves. The scaling procedure employed herein is based on the spectral displacement values at the fundamental period of the structure. The interstory drift values obtained from the dynamic analyses range between 0.14%-0.22%, corresponding to slight-damage in terms of the limit states determined for the building used in the case study. Scale factors to be applied to the ground motions are selected so that the response of the structure can be monitored over a wide range to include all damage states. Dynamic analyses are conducted by subjecting random samples of structures to the ground motion records given in Table 1 at each intensity drift level using the corresponding scale factor.

Development of the Fragility Curves

Response statistics are assessed in terms of interstory drift. The damage versus hazard relationship of the flat-slab structure is illustrated in Figure 5. The damage axis (y-axis) described as the interstory drift is given in millimeters whereas the hazard axis (x-axis) is described as spectral displacement and is also given in millimeters. Each vertical line of scattered data corresponds to an intensity level. The horizontal lines in the figure represent the limit states used in this study and described in terms of interstory drift. From bottom to top, these are the limits for Slight, Moderate, Extensive and Complete damage, respectively.

A statistical distribution is fitted to the data for each intensity level on each vertical line. The lognormal parameters; the mean (λ) and the standard deviation (ξ), are calculated for each of these spectral displacement intensity levels. At each intensity level, the probabilities of exceeding the four limit state are calculated. Figure 6 illustrates the statistical distribution for two different intensity levels (when S_d=30 mm and 60 mm, respectively). LS1, LS2, LS3 and LS4 represent the limit states for Slight, Moderate, Extensive and Complete Damage, respectively, as mentioned above. The mean and standard deviation values of the response data are also given in the figure. The probability of exceedence of a certain limit state is obtained by calculating the area of the lognormal distribution over the horizontal line of that limit state. Hence the following values are obtained for the depicted two intensity levels:

For S_d=30 mm,
$P(S_d > LS1) = 0.999$
$P(S_d > LS2) = 0.404$
$P(S_d > LS3) = 0.083$
$P(S_d > LS4) = 0.011$

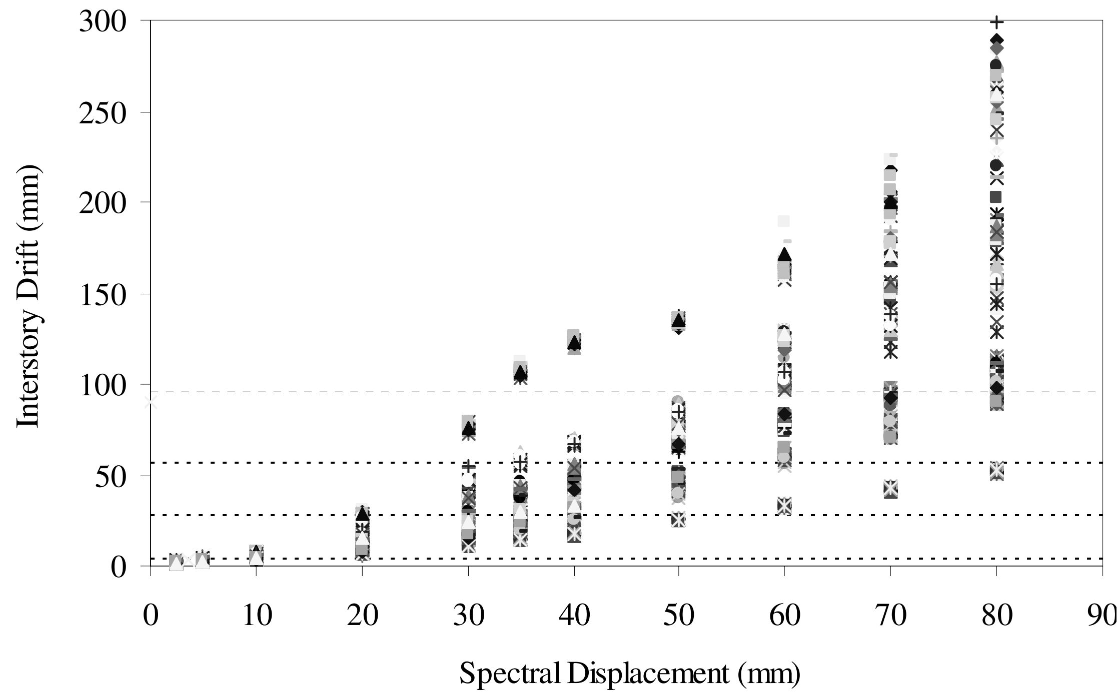

Figure 5. Damage vs. hazard relationship for the flat-slab structure

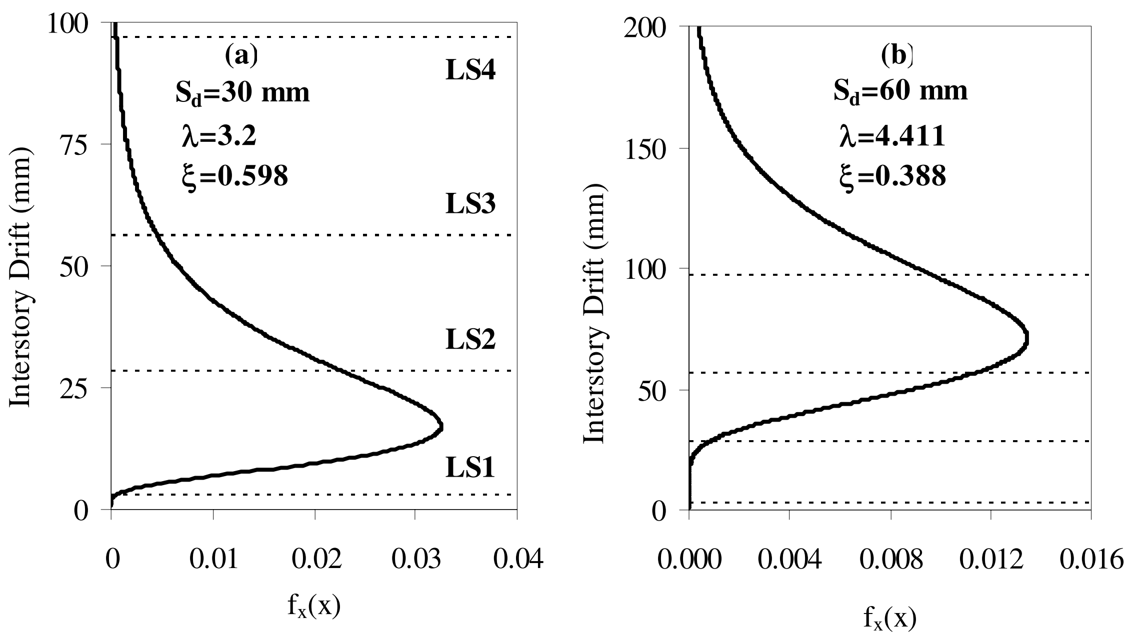

Figure 6. Lognormal statistical distributions for two different levels of seismic intensity; **a)** S_d=30 mm, **b)** S_d=60 mm

For S_d=60 mm,
P (S_d > LS1) = 1.000
P (S_d > LS2) = 0.997
P (S_d > LS3) = 0.839
P (S_d > LS4) = 0.338

After calculating the probability of exceedence of the limit states for each intensity level, the fragility curves can be constructed by plotting the calculated data versus spectral displacement. As the final step, a statistical distribution can be fitted to these data points, to obtain the fragility curves. In this study, a lognormal fit is assumed.

Figure 7 represents the fragility curves of medium rise flat-slab structures. The curves become flatter as the limit state shifts from slight to complete because of the nature of the statistical distribution of the response data. Vertical curves would represent deterministic response. The variability of interstory drift at high ground motion intensity levels is much more pronounced relative to the variability at low intensity levels. Hence small variations in low intensity cause significant differences in the limit state exceedence probabilities. This observation points towards the high sensitivity of the structure to changes in seismic demand. The steep shape of the slight limit state curve is due to the infill panels dominating the response at this low-level limit state. This continues till the panels reach their deformation capacity. Thereafter, the response is dictated by the bare flexible flat slab system.

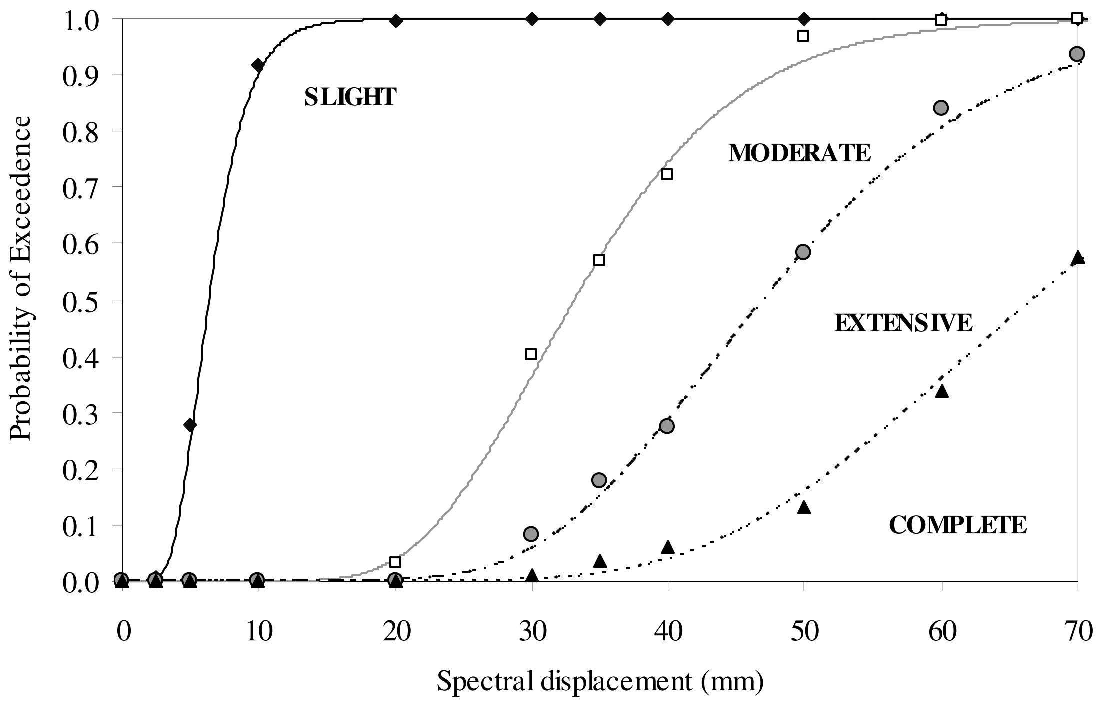

Figure 7. Fragility curves for the flat-slab structure

COMPARISON OF DEVELOPED FRAGILITY CURVES WITH MOMENT-RESISTING FRAMES

The fragility curves of flat-slab structures derived in the previous section require a form of validation, since no experimental or observational data sets have been hitherto used in the derivation. A possible verification approach is to derive vulnerability curves for familiar moment-resisting frames, establish the realism of the latter by comparison with the literature and hence establish the realism of the new flat-slab curves. This was accomplished by developing the mean fragility curves of a framed structure using the same methodology as for the flat-slab structure.

In order to develop the mean fragility curves for the framed structure, modifications were made to the previous analytical model. The slab-beams were replaced by conventional beams of 300 mm x 600 mm and a longitudinal reinforcement ratio ρ of 1.5%. The columns and the infill walls were kept the same as the original flat-slab model. Mean fragility curves for the moment-resisting frame are shown in Figure 8 alongside the fragility curves for flat-slab structures. It is shown that the flat-slab structure is more vulnerable to seismic damage than the moment-resisting frame across the entire range of seismic hazard. It is also interesting to observe that the difference between the flat-slab structure and the framed structure is more pronounced at the lower limit states. This is because of the inherent flexibility of flat-slab structures, as mentioned in previous sections. Small variations at low levels of seismic intensity can create amplified effects on the fragility curves whereas even large variations at high levels of seismic intensity may not have that much effect on the curves.

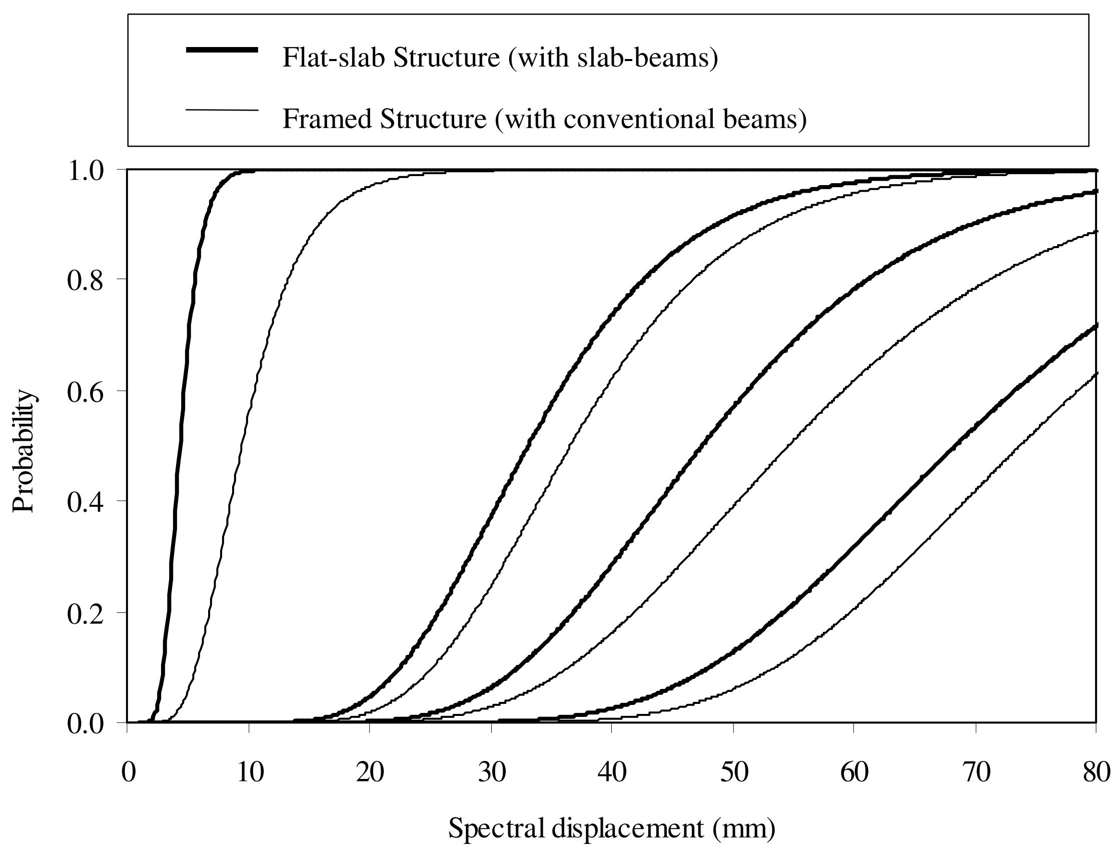

Figure 8. Comparison of fragility curves for flat-slab and framed structures

The next step would be to compare the fragility curves derived for moment-resisting structures to the fragility curves from the literature. This is a challenge because of the dearth of spectral displacement-based vulnerability curves in the literature. Therefore, it was necessary to reconstruct the fragility curves for framed structures using spectral acceleration instead of spectral displacement.

This was accomplished by converting the spectral values and then matching the converted values with the corresponding response (interstory drift) values. The spectral acceleration-based fragility curves are shown in Figure 9. Figures 10 and 11 show the comparison of the curves obtained for framed structures against the curves developed by Hwang & Huo [11] and Singhal and Kiremidjian [12]. For the sake of simplicity, the curves that belong to Hwang and Huo are named as HH curves and the ones that belong to Singhal and Kiremidjian are named as SK curves. The HH curves in Figure 10 were developed for low-rise (1-3 story) concrete frames. Four damage states were considered in terms of maximum interstory drift ratio, ID_{max}: (1) no damage, when $ID_{max} < 0.2\%$, (2) insignificant damage, when $0.2\% < ID_{max} < 0.5\%$, (3) moderate damage, when $0.5\% < ID_{max} < 1.0\%$ and (4) heavy damage, when $ID_{max} < 1.0\%$. More information about these fragility curves are discussed in Table 3. The SK curves in Figure 11 were developed for mid-rise reinforced concrete frames. The Park and Ang damage index was used as the response parameter. Damage states were also identified based on this damage index after calibration with observed damage to several buildings caused by different earthquakes. According to the damage scale, minor damage occurs when the index attains values between 0.1 and 0.2; moderate damage occurs when the index values are between 0.2 and 0.5 and severe damage occurs when the index values are between 0.5 and 1.0. Exceedence of unity for the index value corresponds to the collapse limit state. Additional information about the SK fragility curves is also discussed in Table 3.

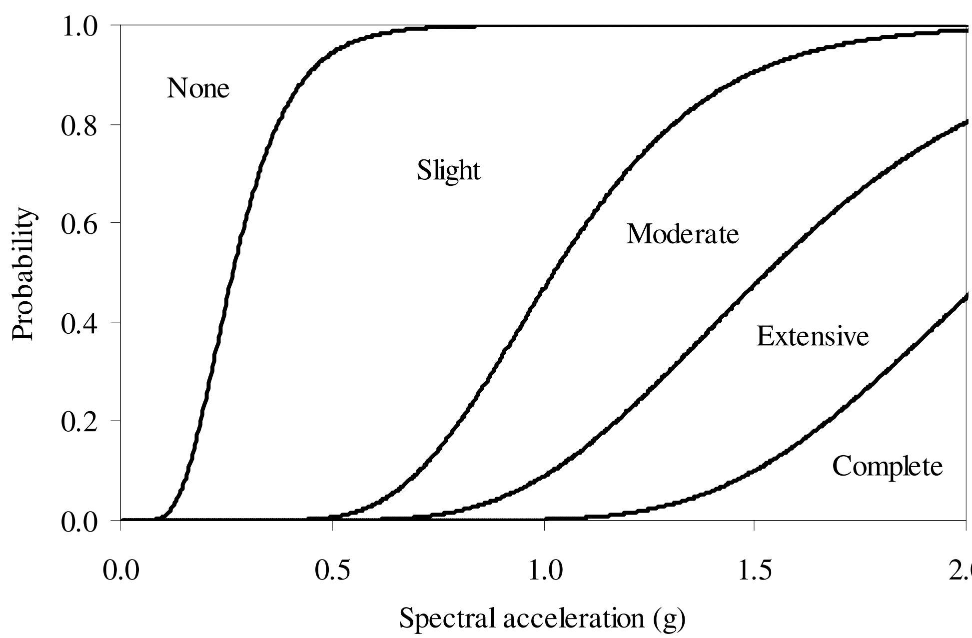

Figure 9. Acceleration-based fragility curves for the framed structure

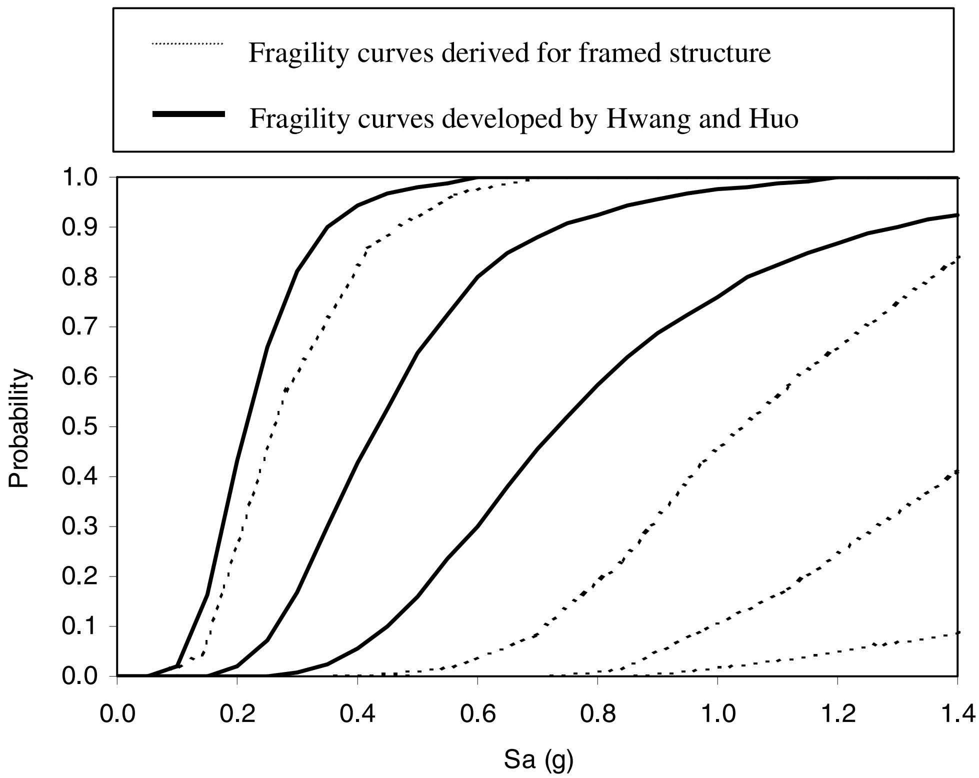

Figure 10. Comparison of the study curves for framed structure with HH curves

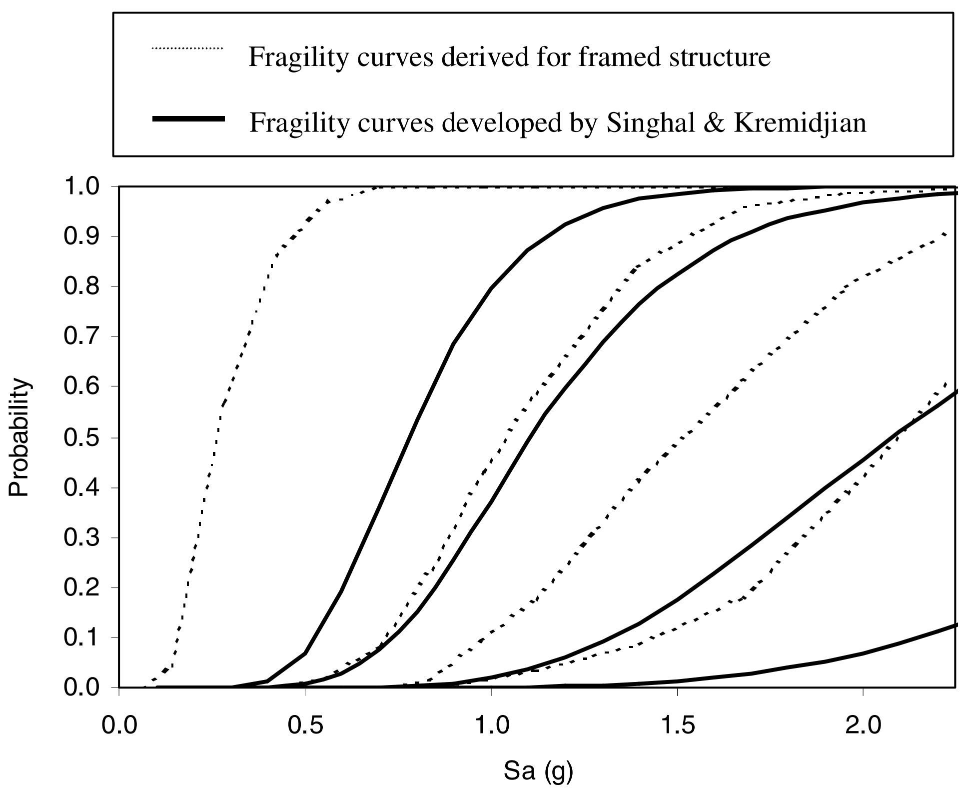

Figure 11. Comparison of the study curves for framed structure with SK curves

Table 3 Comparison of fragility curve characteristics

	Derived Curves	***SK Curves***	***HH Curves***
Structure	RC Frame (MR)	RC Frame (MR)	RC Frame (LR)
Ground Motion	Actual, from various earthquakes	Synthetic (for West US region)	Synthetic (Close to NMSZ)
Analysis Method	Time-history	Time-history	Time-history
Random Variables	f_c, f_y	f_c, f_y	f_c, f_y
Damage Parameter	Interstory Drift	Park & Ang Index	Interstory Drift
Hazard Parameter	Spectral displacement	Spectral acceleration	Spectral acceleration and PGA
Limit States	4	4	3

The fragility curves developed in this study have a better match with the SK curves than with the HH curves. The study curves seem to result in more damage in the case of the SK curves whereas the opposite is true when compared with the HH curves. As seen in Table 3, ground motion selection is quite different. There are also differences in the characterization of the hazard and the damage parameters. Quantification of the limit states of the SK and the HH curves are discussed in the above paragraphs and the values defined for this study are given in Table 2. In general, methods that different researchers adopt to determine fragility curves can cause significant discrepancies in the vulnerability predictions for the same location, even in cases where the same structure and seismicity are considered (Priestley [13]). In a statistical context, the agreement between the vulnerability curves derived above for moment-resisting frames and those of Hwang and Huo [11], and Singhal and Kiremidjian [12] is reassuring and lends weight to the curves derived for flat-slab structures.

SUMMARY AND CONCLUSIONS

The purpose of this research was to develop fragility curves for flat-slab structure system for which no fragility analysis has been undertaken before. A mid-rise flat-slab building is designed and modeled using the structural characteristics typical of flat-slab building. The preliminary evaluation of the structure indicates that the model structure is more flexible than conventional frames because of the absence of deep beams and/or shear walls. The reliability of the newly derived vulnerability curves is underpinned by the quality of the models used, methodology adopted and software employed. Moreover, the same approach and tools are used to derive median curves for moment-resisting frames for which there is an abundance of fragility studies in the literature. Comparison between the flat slab and moment-resisting buildings on the one hand and the latter and two published studies, makes the case of the reliability of the new curves. The curves are recommended to be used for seismic loss assessment in regions where flat slab structures exist. With regard to the characteristics of the flat slab vulnerability curves, they display response features of this special type of construction. The steep light-damage curve reflects the role of the infill panels that dominate the response in the vicinity of the light-damage limit state. When the infill panels are damaged and no longer contribute to the lateral resistance, the buildings violate interstory drift limits more readily than their moment-resisting counterparts. Therefore, using vulnerability curves of moment-resisting frames to assess seismic damage of flat slab buildings in non-conservative.

ACKNOWLEDGEMENTS

The work described in this paper was funded by the Mid-America Earthquake Center through the National Science Foundation Grant EEC-9701785. Additional funding was provided by a postdoctoral fellowship from The Scientific and Technical Research Council of Turkey (TUBITAK). Thanks are extended to

Professors Dan Abrams (University if Illinois at Urbana-Champaign and MAE Center Director) and Joe Bracci (Texas A&M University, and MAE Center investigator) for their constructive comments which helped improve this study. Valuable suggestions were also provided by Professor Haluk Sucuoglu, Middle East Technical University, Turkey. The paper is a product of MAE Center Project DS-9 'Risk Assessment Systems'. Any findings in this paper do not represent the opinion of NSF and the other sponsors or individuals mentioned above.

REFERENCES

1. ACI-ASCE Committee 352, 1988. "Recommendations for Design of Slab-column Connections in Monolithic Reinforced Concrete Structures", ACI Structural Journal, Vol.85, No.6, pp. 675-696.
2. Chow, H. L. and Selna, L. G., 1995. "Seismic Response of Nonductile Flat Plate Buildings", Journal of Structural Engineering, ASCE, Vol.121, No.1, pp. 115-123.
3. Wen, Y.K., Ellingwood, B.E., Veneziano, D. and Bracci, J., 2003, 'Uncertainty Modeling in Earthquake Engineering', Mid-America Earthquake Center Project FD-2 Report.
4. ACI Committee-318, 1999. "ACI 318-99, Building Code Requirements for Structural Concrete", American Concrete Institute, Detroit, Michigan.
5. Building Seismic Safety Council, 2001. NEHRP Recommended Provisions for Seismic Regulations for New Buildings and Other Structures, Part.1 Provisions (FEMA 368), Washington D.C.
6. Elnashai, A.S., Papanikolaou, V. and Lee, D.H., 2002. ZEUS NL User Manual, Civil and Environmental Engineering Department, University of Illinois at Urbana-Champaign.
7. Luo, Y.H., Durrani, A., 1995. "Equivalent Beam Model for Flat-Slab Buildings: Interior Connections", ACI Structural Journal, Vol.92, No.1, pp. 115-124.
8. Erberik, M.A. and Elnashai, A.S., 2004. "Seismic Vulnerability of Flat-Slab Structures", Mid-America Earthquake Center DS-9 (Damage Synthesis Thrust Area) Project Report, Civil and Environmental Engineering Department, University of Illinois at Urbana-Champaign.
9. Bazzuro, P. and Cornell, C. A., 1994. "Seismic Hazard Analysis of Nonlinear Structures I: Methodology", Journal of Structural Engineering, ASCE, Vol.120, No.11, pp. 3320-3344.
10. Dymiotis, C., Kappos, A. J., Chryssanthopoulos, M. K., 1999. "Seismic Reliability of RC Frames with Uncertain Drift and Member Capacity", Journal of Structural Engineering, ASCE, Vol.125, No.9, pp. 1038-1047.
11. Hwang, H. and Huo, J-R., 1997. "Chapter 7.b: Development of Fragility Curves for Concrete Frame and Shear Wall Buildings", Loss Assessment of Memphis Buildings, Technical Report NCEER 97-0018, pp 1136-137.
12. Singhal, A. and Kiremidjian, A.S., 1997. "A Method for Earthquake Motion-Damage Relationships with Application to Reinforced Concrete Frames", Technical Report NCEER 97-0008, National Center for Earthquake Engineering Research, Buffalo, NY.
13. Priestley, M.J.N., 1998. "Displacement Based Approaches to Rational Limit States Design of New Structures", Proceedings of the 11th European Conference on Earthquake Engineering, A.A. Balkema, Rotterdam.